Journal of Global Engineering Research & Science (J-GERS)
Vol. 05, No. 01, June 2026, pp. 10-20
ISSN: 2830-5906, *e*-ISSN: 2830-5418, DOI: 10.56904/j-gers.v5i1.200

Dynamic Interaction of Bridge Spans and Piers as a Tuned System for Seismic Load Reduction

Ziyovuddin Rahimjonov [1], Fakhriddin Zokirov[1*], Lintang Dian Artanti[2]
[1*] Department of Bridge & Tunnel, Tashkent State Transport University, Temiryo'lchilar Street 1, Tashkent 100167, Uzbekistan
[2]Department of Civil Engineering, Faculty of Engineering & Computer Science, Jakarta Global University, Indonesia, 16412

Article Info

Article history:

Received May 06, 2026
Revised June 24, 2026
Accepted June 29, 2026

Keywords:

Seismic protection
Bridge pier
Dynamic vibration absorber
Seismic response reduction
Two-degree-of-freedom system

ABSTRACT

Bridges located in seismic regions are subjected to significant dynamic loads that may cause considerable forces in bridge piers and foundations. Traditional seismic design methods usually consider the span structure as a rigid mass transferring inertial forces to the supports. However, this approach does not account for the potential dynamic interaction between the span and the supporting structure. This study proposes a method for reducing seismic forces in bridge piers by using the span structure as a tuned dynamic system. In the proposed approach, the bridge span is considered as a dynamic vibration absorber interacting with the pier. A mathematical model based on a two-degree-of-freedom system is developed to describe the dynamic behavior of the bridge–pier system under seismic excitation. Parametric analysis is carried out to determine the optimal stiffness and damping parameters that minimize seismic forces in the pier. The results show that appropriate tuning of the span structure significantly reduces dynamic responses. In particular, the bending moment in the bridge pier can be reduced by up to 2.3 times compared with traditional seismic design approaches. The proposed method can be applied in seismic regions for improving the seismic performance and reliability of bridge structures.

Corresponding Author:

Fakhriddin Zokirov
Department of Bridge & Tunnel, Tashkent State Transport University, Temiryo'lchilar Street 1, Tashkent 100167, Uzbekistan
Email: zokirov_f@tstu.uz

1. INTRODUCTION

Reinforced concrete bridges located in seismically active areas have a high sensitivity to the effects of earthquakes due to their large mass, the concentration of inertia forces in the supporting elements, and structural irregularities [1], [2]. Observations after strong earthquakes show that bridge supports and supporting parts are the weakest elements that determine the overall seismic stability of the structure [3], [4]. Excessive bending moments, shear forces, and displacements arising in these elements can lead to structural damage, shutdown, or emergency situations [3].

Traditional approaches to bridge seismic protection generally rely on three main directions: (1) increasing the strength and rigidity of the structure, (2) redistributing seismic forces between several load-bearing elements, and (3) applying seismic isolation and additional damper devices[5], [6]. In practice, seismic isolation systems and external dynamic dampers are widely used, since they reduce the load on the supports by extending the vibration period of the structure and increasing energy dissipation[7], [8]. However, such systems often cause large relative shifts, increase structural complexity, and increase operating costs. At the same time, the mass of the large span structure, which is present in multi-span bridges, is not used as the total dynamic potential. As an alternative approach, the concept of using the bridge span itself as a dynamic vibration damper (VDD) for the support can be proposed. Unlike classical adjustable mass dissipators, this approach does not require additional mass but is based on the efficient use of the mass of the existing intermediate device[9]. In this case, the redistribution of seismic energy and the reduction of support vibrations are ensured by the targeted selection of stiffness and damping parameters between the span structure and the support. At the same time, most current research is devoted to models of ideal adjustable mass dampers used in traditional seismic isolation systems or buildings. In multi-span reinforced concrete bridges, especially in cases where the ratio of the mass of the span structure to the mass of the support is significantly large, the mechanism of dynamic interaction of the system has not been sufficiently studied. Under these conditions, the direct application of classical TDS theory is insufficient, and it is necessary to develop an optimization process based on dimensionless parameters. In this study, an improved approach is proposed, based on the use of a bridge span as an effective dynamic damper for the support. A dimensionless model of a system with two degrees of freedom has been developed, and a methodology for determining the optimal stiffness and damping parameters based on minimizing the amplitude-frequency characteristic of support displacements has been developed. The proposed method is implemented within the framework of linear spectral calculations and is tested using the example of a multi-span reinforced concrete bridge located in a seismic zone. The results show that by purposefully adjusting the span-support interaction, it is possible to significantly reduce bending moments in the supports, while maintaining practically acceptable displacement limits.

2. MATERIAL AND METHODS

2.1. Statement of the problem

In this study, an improved method for calculating multi-span reinforced concrete bridge structures for seismic impacts is based on the consideration of span structures as dynamic vibration dampers, in which displacements and stresses at characteristic points of the structure under seismic loads are determined based on the second form of vibration. In this case, the mass of the support (m_{pier}) and the mass of the span (m_{span}) are expressed through stiffness coefficients (k_{pier} and k_{iso}) and damping stiffness (C_{span} and C_{iso}), respectively [10].

The equation of motion of the system is summarized as follows:

$$M\ddot{q} + C\dot{q} + Kq = -Mr\ddot{u}_g(t) \tag{1}$$

where: $\ddot{u}_g(t)$ – ground acceleration, M, C, K - mass, attenuation, and stiffness matrices, respectively.

It is expressed using dimensionless parameters as follows:

$$\mu = \frac{m_{span}}{m_{pier}}, f = \frac{k_{iso}}{k_{pier}}, \gamma = \frac{C_{iso}}{C_{span}} \tag{2}$$

where: μ – mass ratio;
f – relative stiffness parameter of insulation;
γ – attenuation factor.

The purpose of the research is to determine the parameters of the optimal insulation stiffness (f) and damping coefficient (γ), minimizing support displacements and bending moments based on the minimization of the amplitude frequency characteristic. In the optimization process, the displacement of the span structure relative to the support is limited by practical operational limitations.

2.2. Existing calculation methods

The scientific development of the theory of bridge seismic resistance dates to the beginning of the 20th century. The theory of seismic resistance of modern structures was developed by such scientists V.A. Ilyichev[11], S.V. Medvedev[12], T.R. Rashidov[13], A.M. Uzdin[14], and many others. According to the static approach proposed by Fusakichi Omori [15], the inertial force acting on the structure is proportional to its mass and the acceleration of the Earth's horizontal oscillations.

$$F = m \cdot a \tag{3}$$

This method is known as the "theory of static equivalent seismic forces" and allows for quick and simple assessment of the seismic load on buildings and ordinary structures. At the same time, since this approach does not fully reflect the actual dynamic behavior of structures, more advanced dynamic methods have been developed.

In 1933, Maurice Biot proposed determining the seismic resistance of buildings and structures using a dynamic calculation method based on spectra [16]. This approach made it possible to assess seismic impacts accurately and in accordance with their physical content.

$$F = m \cdot S_a(T) \tag{4}$$

In this method, the amplitude-frequency spectrum of the earth's oscillation process is compared with the natural oscillation period of the structure, and as a result, the values of maximum acceleration, maximum velocity, and maximum displacement of the structure are determined. This made it possible to fully consider the real dynamic nature of the earthquake's impact compared to traditional methods based on statically

e-ISSN: 2830-5418, p-ISSN: 2830-5906

equivalent forces.

The approach, developed by Japanese scientists Toshikatsu Mononobe and Matsuo Okabe, is distinguished by the application of a model of a cantilever rod with a point support to the base of the structure [17]. The seismic motion of the base is described by a sinusoidal law, and the elastic properties of the system are considered [18].

$$\beta(\eta) = \frac{1}{1-\eta^2} \tag{5}$$

As a result, a dynamic coefficient was introduced when assessing the seismic load, which is derived from the frequency ratio of the system and the harmonic oscillation of the base. At the same time, the Mononobe-Okabe model was developed mainly for retaining walls, dams, and slopes, which served as a theoretical basis for the further development of the dynamics of seismic structures.

Currently, in the Republic of Uzbekistan, the regulatory document QMQ 2.01.03-19 “Construction in Seismic Areas” is used in the design of structures in seismic zones. In this norm, the dynamic response of buildings and structures is assessed depending on the soil conditions, the typology of the structure, and the forms of natural vibrations [19].

$$S_{ik} = K_0 \cdot K_n \cdot K_{et} \cdot K_p \cdot S_{oik} \tag{6}$$

$$S_{oik} = \alpha \cdot Q_k \cdot W_i \cdot K_\delta \cdot \eta_{ik} \tag{7}$$

That is, QMQ 2.01.03-19 is adapted to modern seismic design, combining the scientific foundations of historical approaches (Omori, Biot, Mononobe-Okabe).

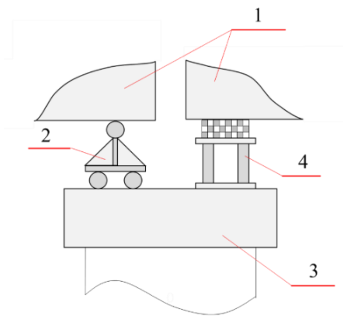

Figure. 1. Simple seismic isolation: 1 - span structure, 2 - movable support part, 3 - support head, 4 - flexible support part

The above-mentioned scientific approaches, spectral analysis, and regulatory framework are of great importance in assessing the seismic state of structures and create an important scientific and practical basis for ensuring the seismic stability of structures, in particular, bridges on highways. Since bridges, as the main elements of transport infrastructure, have specific features in relation to seismic phenomena, the development of effective protection systems for them is an urgent task. The simple seismic protection characteristic of bridges on highways in seismically active areas implies the construction of flexible seismic isolation support sections on each support instead of traditional fixed support sections (Fig. 1).

The strategy for selecting the parameters of simple seismic isolation depends on the ratio calculated according to the following formula.

$$\nu = M_{span}/M_{pier} \tag{8}$$

The mass of the support is calculated as follows.

$$M_{pier} = C_0/k_0^2 \tag{9}$$

Where: C_0 - bending stiffness of support;

k_0^2 - oscillation frequency of a support without an intermediate structure.

In cases where the ratio of the mass of the span structure to the mass of the support (according to formula 6) is less than 2, the optimal option for stiffness and damping of the flexible support part is selected. In this case, the intermediate structure acts as a dynamic vibration damper (DDS). Conversely, in cases where the ratio of the mass of the span structure to the support mass is greater than 2, it is impossible to choose the optimal option. In this case, it is advisable to make the insulating support parts as flexible as possible [20]. In this case, it is necessary to ensure the strength of the insulating support part and the displacement of the movable support part.

3. RESULTS AND DISCUSSION

3.1. Seismic protection and damping approaches for bridges

The object of the research is the highway bridge over the Chirchik River, which flows through the Tashkent region of the Republic of Uzbekistan. The seismicity of the territory is taken as 7, 8, and 9 points according to the Figure 2.

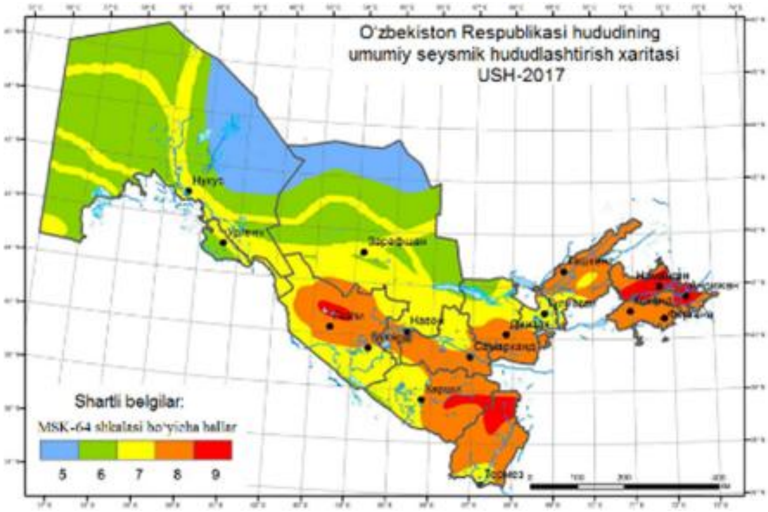

Figure 2. General seismic zoning map of territory of Uzbekistan

In the development of project documentation, the principle of multi-stage design has been adopted, allowing for the following limiting cases:

1. Weak earthquakes can occur once every 475 years.
2. Catastrophic earthquakes can occur once every 5000 years, the displacement of the span structure relative to the support is assumed to be no more than 100 mm.

There are the following methods for accepting seismic loads in bridge structures:

1. Strengthening of structures that directly accept seismic loads;
2. Redistribution of seismic forces;
3. Seismic protection;
4. Seismic damping.

The first approach is considered a traditional method, based on the need to accept active seismic loads, the sections of structural elements are improved. The second approach is the redistribution of seismic forces into many elements, i.e., for single-span schemes, longitudinal seismic forces can be redistributed into two supports, which reduces seismic forces. The third approach is the seismic protection of span structures from supports, in which the energy of seismic vibrations is redistributed into kinetic or thermal energy. The fourth approach is the calculation of seismic vibration damping using dynamic dampers, and a structural connection of a certain stiffness is established between the span structure and the support. An intermediate structure, oscillating in the opposite phase relative to supports or other intermediate structures, can be used as a vibration damper.

3.2. Selection of elastic damping parameters of seismic protection support parts

The considered methods of fastening span structures are presented in Figure. 3, reduced to simple calculation schemes of the support. The first two circuits have two degrees of freedom, and the next two circuits have three degrees of freedom. In the figure, the blue circles represent concentrated structural masses or connection points, the zigzag lines indicate elastic or seismic isolation elements, and the vertical members represent the supporting columns or piers. Scheme (a) illustrates a structure equipped with seismic protection combined with a rigid support, where horizontal movement is restrained to provide high structural stability. Scheme (b) shows seismic protection combined with a movable support, allowing controlled displacement and reducing the transmission of seismic forces to the structure. Scheme (c) represents a configuration in which seismic protection elements are installed on both sides of the structure, providing improved vibration reduction and more uniform energy dissipation during earthquake loading. Meanwhile, scheme (d) combines seismic protection with an additional spring element and movable support, increasing structural flexibility and damping capacity under dynamic excitation. Overall, the figure demonstrates how different support and isolation configurations influence the seismic behavior and vibration response of span structures

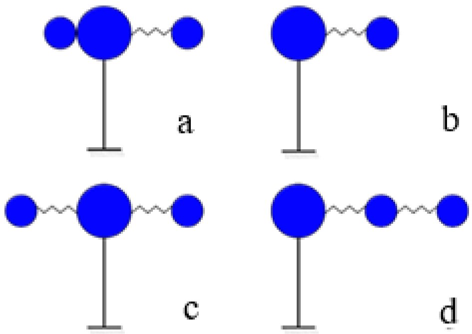

Figure. 3. Calculation schemes of span structures in various connections with supports, a - seismic protection + rigid support part; b - seismic protection + movable support part; c - seismic protection + seismic protection; d - seismic protection + spring + movable support part

Optimal parameters for each variant are selected in accordance with the stiffness coefficient C and the inelastic resistance coefficient γ of the connecting element of the span structure with the support. The amplitude-frequency characteristic (AFC) is determined using the standard method for parameter selection, where the relative displacements in the grid are minimal. For the calculation of displacements, the following equation proposed in is used [21]:

$$\boldsymbol{M}\ddot{\boldsymbol{q}} + \boldsymbol{B_c}\widetilde{\boldsymbol{q}} + \boldsymbol{Rq} = \boldsymbol{P}\sin\omega t, \tag{10}$$

where:
$\boldsymbol{B_c}$ – is the hysteresis damping matrix;
$\boldsymbol{M}$ – is the inertia matrix;
$\boldsymbol{R}$ – is the stiffness matrix;
$\boldsymbol{P}$ – is the effect amplitude vector;
$\boldsymbol{\omega}$ – is the forced oscillation frequency;
$\boldsymbol{q}$ – is the displacement vector;
$\widetilde{\boldsymbol{q}}$ – is the complex conjugate vector.

The matrix $\boldsymbol{B_c}$ is determined by replacing the modulus of elasticity with $\boldsymbol{\gamma E}$ according to the hypothesis of E.S. Sorokin [22]. In practical calculations, it is often replaced by an equivalent viscous damping matrix:

$$\boldsymbol{B_e} = \boldsymbol{B_C} \cdot \boldsymbol{X} \cdot \boldsymbol{K^{-1}} \cdot \boldsymbol{X^{-1}} \tag{11}$$

where:
$\boldsymbol{X}$ – is the matrix of eigenvectors of the undamped system;
$\boldsymbol{K}$ – is the diagonal matrix of eigenvalues.

As a result, the system equation is written as follows:

$$\boldsymbol{M}\ddot{\boldsymbol{q}} + \boldsymbol{B_e}\dot{\boldsymbol{q}} + \boldsymbol{Rq} = \boldsymbol{P}\sin\omega t \tag{12}$$

If the substitution of hysteresis damping with viscous damping gives a large error, then both types of damping are considered in the system. The solution to the equation is taken as the sum of sine and cosine:

$$\boldsymbol{q} = \boldsymbol{S}sin\omega t + \boldsymbol{C}cos\omega t \tag{13}$$

For the resulting system of equations, the formulas proposed in were used to reduce errors in the resonance domain. On this basis, the amplitude of the support oscillations and the APV were minimized for different values of C and γ. To simplify optimization, the equations were reduced to dimensionless form, and the following parameters were introduced:

$$\nu_i = \frac{m_i}{m_0} \qquad f_i = \frac{k_i}{k_0} \qquad k_0 = \frac{c_0}{m_0}$$

Optimal parameters were selected by the stiffness of the protective support parts f_1, f_2, and the damping coefficients γ_1, γ_2. In this case, the displacement of the span structure relative to the support was limited by the condition of operation of the deformation joints. Ultimate displacement under static load:

$$S_i = m_i \cdot Ag, \tag{14}$$

and the limiting displacement:

$$u_{lim} = \frac{S_i}{C_i} = \frac{Agm_i}{C_i} = \frac{Ag}{k_i^2}, \tag{15}$$

from which the minimum stiffness of the protective support parts is determined. For the calculations, the dynamic parameters of the individual support were determined:

$$T_0 = 0.314\ s; \qquad k=3,18\ s^{-1}; \qquad \delta_{1,1} = 2\cdot 1.8328\cdot 10^{-4}\ m.$$

Accordingly, the reduced mass of the support is equal to m = 271.200 N. The mass of the span structure is quite large, $\nu_1=\nu_2=492.600$ N amounted to.

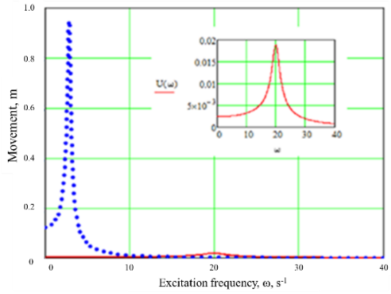

Figure. 4. Oscillations of the upper part of the support without an intermediate structure and with an intermediate structure

Figure 4 illustrates the oscillation response of the upper part of the support structure under varying excitation frequencies, comparing the behavior of the system without an intermediate structure and with an intermediate structure. The graph shows that, without the intermediate structure, the oscillation amplitude increases sharply and reaches a significant resonance peak at a low excitation frequency, indicating high structural sensitivity to dynamic loading. In contrast, the presence of the intermediate structure substantially reduces the amplitude of oscillation and shifts the vibration response to a more controlled range. The inset graph further highlights the reduced resonance behavior, demonstrating that the intermediate structure acts as a vibration damping or seismic isolation component that effectively minimizes excessive movement and improves the dynamic stability of the support system under excitation.

The use of a single span structure as seismic insulation does not correspond to the critical mass $\nu\approx2$ required for a dynamic damper.

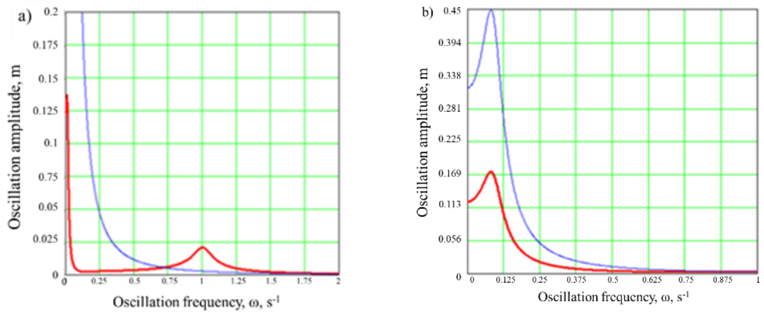

a) f = 0.01 b) f = 0.075

Figure. 5. AFC of the system with excessive seismic isolation flexibility

The graphs illustrate in figure 5 is the relationship between oscillation amplitude and excitation frequency, showing how the system responds dynamically under varying damping levels. In both cases, the oscillation amplitude reaches a peak near the natural frequency of the system, indicating resonance behavior. For the lower damping coefficient in Figure 5(a), the system experiences sharper resonance peaks and larger oscillation amplitudes, reflecting reduced energy dissipation and greater vibration sensitivity. In contrast, Figure 5(b) demonstrates that increasing the damping coefficient reduces the resonance intensity and smooths the response curve, thereby improving vibration control and structural stability. Overall, the results indicate that excessive flexibility in seismic isolation systems can significantly influence resonance characteristics, while adequate damping helps minimize excessive oscillatory response during dynamic excitation. Therefore, the limitation of displacements was determined based on the capabilities of the deformation joints. For the considered bridge, the permissible displacement of the span structure relative to the support was taken as 6-12 cm.

Figure 6 illustrates the relationship between oscillation amplitude and excitation frequency, representing the dynamic response of the structure under seismic loading conditions. In both cases, the oscillation amplitude increases near the resonance frequency and gradually decreases as the excitation frequency moves away from resonance. In Figure 6(a), the lower damping coefficient produces a higher and broader resonance peak, indicating greater vibration sensitivity and larger structural displacement. Meanwhile, Figure 6(b) demonstrates that increasing the damping coefficient results in a more controlled response, characterized by reduced oscillation amplitudes and improved vibration attenuation.

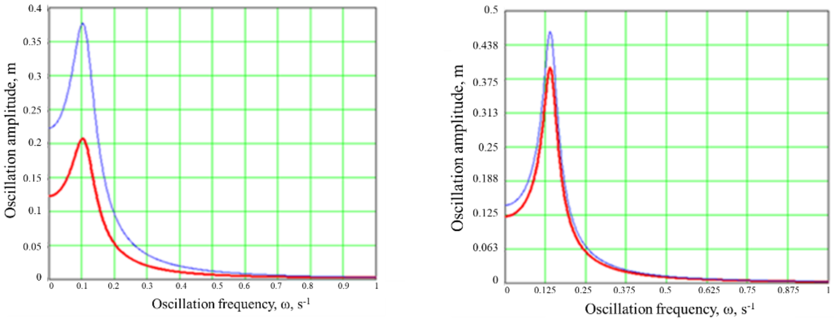

a) f = 0.1; b) f = 0.2.

Figure. 6. AFC of system vibrations with optimal seismic isolation stiffness

The analysis further shows that the effectiveness of seismic isolation strongly depends on the stiffness and damping parameters of the system. When the stiffness is very small, structural displacements increase significantly, whereas increasing the stiffness reduces the displacement response but also decreases the effectiveness of seismic load reduction. At $f = 0.1$, the second resonant maximum disappears from the amplitude–frequency characteristic of the system, indicating improved vibration control. Overall, the results suggest that optimal seismic isolation stiffness combined with adequate damping can effectively reduce resonance effects, enhance energy dissipation, and improve the overall dynamic stability of the structural system during seismic excitation.

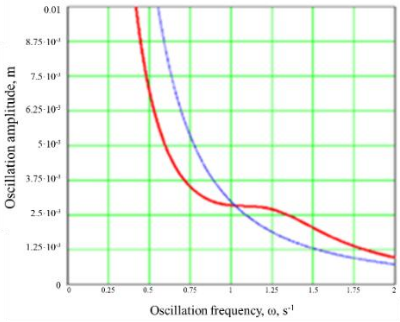

Figure. 7. Loss of the second resonant maximum in the AFC of the system

Figure 7 illustrates the loss of the second resonant maximum in the amplitude–frequency characteristic (AFC) of the system. The graph shows the relationship between oscillation amplitude and excitation frequency, demonstrating the dynamic behavior of the structure under varying damping and stiffness conditions. As the excitation frequency increases, the oscillation amplitude decreases gradually, and the second resonant peak disappears, indicating improved vibration control and greater system stability. The results show that at $\nu > 2$, the selection of optimal stiffness depends primarily on the damping value. According to the calculation results, achieving optimal structural displacements requires a damping parameter of $\gamma > 1$, which is approximately 50% greater than the critical value. This behavior indicates that adequate damping plays a significant role in suppressing resonance effects, reducing excessive oscillations, and improving the effectiveness of the seismic isolation system during dynamic excitation.

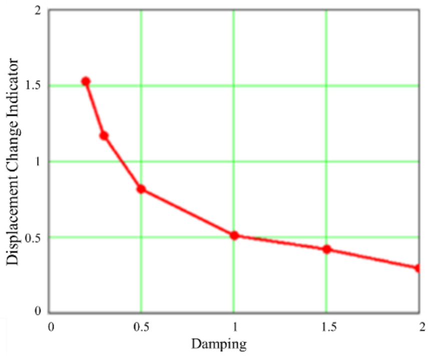

Figure. 8. Dependence of the displacement of the span structure on the damping of the TDS in the AFC

Figure 8 illustrates the relationship between the displacement change indicator of the span structure and the damping coefficient of the TDS in the AFC system. The graph shows that the displacement indicator decreases significantly as the damping value increases from 0.12 to 2.0, indicating that the seismic insulation system becomes more stable with higher damping values. The steep decline in the curve between damping values of 0.12 and 0.5 indicates that small increases in damping at the lower range have a substantial influence on reducing structural displacement. After the damping value reaches approximately 1.0, the curve becomes flatter, showing that additional damping provides only minor improvements in displacement reduction. This behavior demonstrates that the system response becomes less sensitive to damping changes at higher values. The results also indicate that the TDS effectively absorbs and dissipates seismic energy, thereby limiting excessive movement of the span structure during dynamic excitation. Therefore, the selection of an appropriate damping coefficient is essential to ensure efficient seismic performance while avoiding unnecessary increases in system stiffness or energy dissipation capacity.

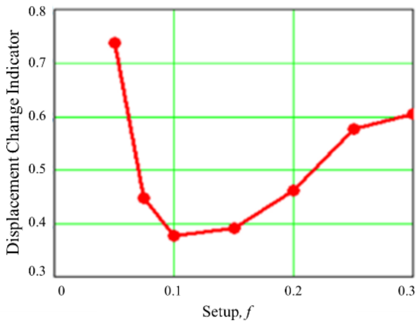

Figure. 9. Relationship between the displacement of the intermediate structure and the upper part of the support and the adjustment of the insulation by stiffness (at damping γ=2)

Figure 9 illustrates the relationship between the displacement of the intermediate structure and the upper part of the support with respect to the adjustment of insulation stiffness at a constant damping value of $\gamma = 2$. The graph shows that the displacement changes indicator decreases sharply at the initial stage as the stiffness adjustment parameter $f$increases from 0.05 to approximately 0.10. The minimum displacement value is observed near $f = 0.10$, indicating the optimal stiffness adjustment condition for achieving effective seismic isolation performance. This result suggests that an appropriate increase in insulation stiffness can significantly reduce the relative displacement between structural components and improve structural stability during seismic excitation. However, after the value of $f$exceeds 0.10, the displacement indicator gradually increases again, indicating that excessive stiffness adjustment reduces the effectiveness of the seismic isolation system. This behavior occurs because overly stiff insulation causes the intermediate structure and support to respond more synchronously to dynamic loading, thereby decreasing the ability of the system to isolate and dissipate seismic energy. In addition, the trend demonstrates that there is an optimum range of stiffness adjustment where the balance between flexibility and rigidity can be achieved effectively. Therefore, proper tuning of the insulation stiffness is essential to minimize structural displacement and maintain efficient vibration isolation performance under seismic loading conditions.

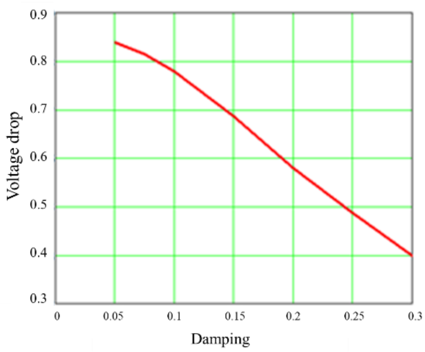

Figure. 10. Dependence of the effectiveness of reducing bearing stresses on the adjustment of seismic insulation

Figure 10 illustrates the dependence of the effectiveness of reducing bearing stress on the adjustment of seismic insulation under harmonic excitation. The graph shows that the voltage drop indicator gradually decreases as the damping parameter increases from 0.05 to 0.30, indicating an improvement in the performance of the seismic insulation system in reducing structural stresses. At lower damping values, the stress reduction effect is less significant due to the limited energy dissipation capability of the insulation system. As the damp adjustment increases, the system becomes more effective in minimizing the transmission of dynamic loads from the support to the span structure. The results indicate that the optimal adjustment range is within f=0.2–0.3, where the bearing stresses can be reduced by nearly two times compared to the initial condition. In this range, the insulation system achieves a more balanced interaction between structural flexibility and damping performance, leading to improved vibration isolation efficiency. Therefore, proper adjustment of seismic insulation parameters is essential to enhance structural safety and reduce the impact of harmonic and seismic loading on the supporting components.

When calculating the seismic isolation system by the linear-spectral method, considering modal attenuation in the system, the calculated isolation efficiency will be sufficiently high. Table 1 presents the dynamic characteristics of support with an intermediate structure with simple and seismically protective support parts according to the first three forms of vibration. The coefficient of inelastic resistance in the support is assumed to be 0.07. For seismic isolation f=0.142; =1.1 values are taken.

Table 1. Dynamic characteristics of span support

Vibration patterns		1	2	3
Period, T, s.	unprotected	0.862	0.076	0.020
	protected	1.011	0.205	0.059
Frequency *k*, rad/s	unprotected	7.60	81.03	319.6
	protected	6.21	30.6	106.4
Inelasticity coefficient γ	unprotected	0.073	0.082	0.077
	protected	0.34	0.67	0.12

The dynamic characteristics presented in Table 1 highlight the significant differences between unprotected and seismically protected span supports across the first three vibration modes. The most notable observation is the increase in vibration periods for the protected system (1.011 s, 0.205 s, and 0.059 s) compared to the unprotected system (0.862 s, 0.076 s, and 0.020 s). This extension of the vibration period indicates that seismic isolation effectively shifts the structural response to lower frequency ranges, thereby reducing the acceleration demands imposed by seismic excitation. Correspondingly, the natural frequencies of the protected support are considerably lower (6.21 rad/s, 30.6 rad/s, and 106.4 rad/s) than those of the unprotected support (7.60 rad/s, 81.03 rad/s, and 319.6 rad/s). This reduction in frequency demonstrates the ability of the isolation system to decouple the structure from high-frequency ground motions, which are typically more damaging to rigid systems. Another critical parameter is the inelasticity coefficient (γ). The protected support exhibits substantially higher values (0.34, 0.67, and 0.12) compared to the unprotected support (0.073, 0.082, and 0.077). This increase reflects the enhanced energy dissipation capacity of the protected system, allowing it to undergo larger deformations without significant loss of stability. Such behavior is essential for mitigating seismic forces and prolonging the service life of the structure. Taken together, these results confirm that seismic isolation improves structural resilience by lengthening vibration periods, lowering natural frequencies, and increasing inelastic energy absorption. The combined effect of these parameters leads to a more efficient seismic response, reducing the likelihood of severe damage under strong ground motions. Therefore, the adoption of seismically protective supports represents a robust strategy for enhancing structural safety and performance in earthquake-prone regions.

Figure 11 illustrates the distribution of bending moments in the support structure under two different conditions: (a) without seismic isolation and (b) with seismic isolation. The vertical axis represents the coordinates of the calculated sections in meters, while the numerical values along the red line indicate the magnitude of the bending moments in kN·m. In Figure 11(a), which represents the structure without seismic isolation, the bending moment values increase significantly from the upper section toward the lower section of the support. The maximum bending moment reaches approximately 1535.1 kN·m at the lower part of the support, indicating that the structure experiences large internal forces under seismic loading. This condition may lead to higher stress concentrations and increase the risk of structural damage during an earthquake. Meanwhile, Figure 11(b) shows the bending moment distribution when seismic isolation is applied. The results demonstrate a substantial reduction in bending moment values throughout the support structure. The maximum bending moment decreases to approximately 657.302 kN·m, which is considerably lower compared to the nonisolated condition. The reduction in bending moments indicates that the seismic isolation system effectively absorbs and dissipates seismic energy before it is transferred to the main structure.

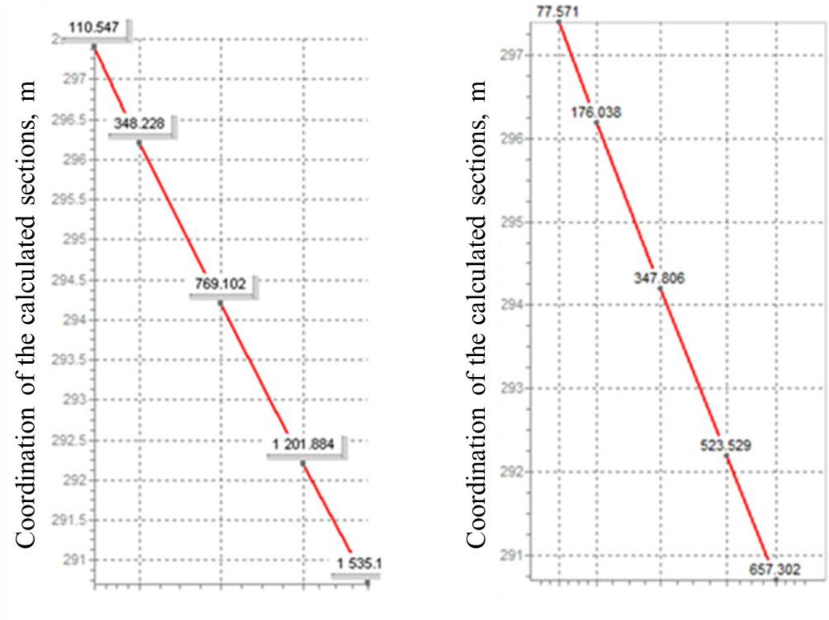

(a) (b)

Figure. 11. Diagram of bending moments in a support (a) without seismic isolation and (b) with seismic isolation (in kN.m)

Overall, the comparison between the two diagrams confirms that the use of seismic isolation significantly improves the structural performance by reducing internal forces and minimizing the effect of earthquake-induced vibrations. This reduction contributes to enhanced structural safety, lower stress on support elements, and improved durability of the structure during seismic events.

4. CONCLUSION

In this study, the dynamic interaction of the bridge span and the support under the influence of an earthquake was analyzed, and the possibility of using the span as an adjusted dynamic system was studied. In traditional seismic calculation methods, the bridge span is considered only as a solid mass transmitting inertial forces to the supports. In this work, the possibility of using the mass of the span structure as a dynamic element that reduces vibrations acting on the bridge support was considered.

During the research, a mathematical model of a bridge span and a support with two degrees of freedom was constructed, and dynamic processes under the influence of an earthquake were analyzed. Based on the calculation results, the optimal values of the stiffness and damping parameters between the span structure and the support were determined, and it was shown that these parameters significantly reduce the dynamic loads acting on the support by controlling the resonant properties of the system.

The obtained results showed that with the correct adjustment of the dynamic parameters of the bridge span and support, bending moments in the support can be reduced by approximately 2.3 times compared to traditional calculation methods. This is important for increasing the seismic stability of bridge structures, ensuring their reliability and operational safety. The proposed approach does not require additional masses or complex extinguishing devices. Therefore, it is economically efficient and can be used in the process of designing and reconstructing bridges located in earthquake-prone areas.

ACKNOWLEDGEMENTS

The authors would like to express their sincere gratitude to Tashkent State Transportation University and Jakarta Global University for their invaluable support and contribution to this research. The facilities, resources, and academic environment provided by the university have greatly facilitated the completion of this study.

REFERENCES

[1] S.-Q. Li, P.-C. Chen, L.-L. Zheng, C. Zhang, P.-F. Qin, and G. Milani, "Seismic failure and risk estimation of reinforced concrete bridges considering fatigue and seismic intensity measures," *Reliability Engineering & System Safety*, vol. 267, p. 111854, Mar. 2026, doi: 10.1016/j.ress.2025.111854.

[2] C. Raupov, A. Karimova, F. Zokirov, and Y. Khakimova, "Experimental and theoretical assessment of the long-term strength of lightweight concrete and its components under compression and tension, taking into account the macrostructure of the material," *E3S Web of Conferences*, vol. 264, p. 02024, Jun. 2021, doi: 10.1051/e3sconf/202126402024.

[3] Y. Hong, L. Ye, and W. Xie, "Seismic fragility and resilience improvement of conventional bridges supported by double-column piers utilizing shear links," *Structures*, vol. 57, p. 105309, Nov. 2023, doi: 10.1016/j.istruc.2023.105309.

[4] S. Salikhanov, Z. Pulatova, F. Zakirov, Z. Rahimjonov, and A. Abdullayev, "Determination of deformations and self-stress in concrete on stress cement," *E3S Web of Conferences*, vol. 264, p. 02056, Jun. 2021, doi: 10.1051/e3sconf/202126402056.

[5] F. Temimi, A. Obaidi, and N. Ermoshin, "Seismic Resilience Assurance and Global Strategies for Highway Bridges," 2026, pp. 45–59. doi: 10.1007/978-3-032-17317-1_4.

[6] M. Berdibaev, B. Mardonov, N. Nishonov, and Z. Rakhimjonov, "Beam vibration due movement of overweight cargoes on reinforced concrete bridges at different ground conditions," *E3S Web of Conferences*, vol. 401, p. 01075, Jul. 2023, doi: 10.1051/e3sconf/202340101075.

[7] X. Xu *et al.*, "Energy dissipation and seismic response reduction system for high-speed railway bridges based on multiple performance requirements," *Engineering Structures*, vol. 307, p. 117919, May 2024, doi: 10.1016/j.engstruct.2024.117919.

[8] S. S. Salixanov, F. Z. Zokirov, Y. T. Xakimova, and G. B. Ismailova, "The effect of increasing loads on foundations of operating bridges," *E3S Web of Conferences*, vol. 401, p. 01080, Jul. 2023, doi: 10.1051/e3sconf/202340101080.

[9] J. Wei, W. Liu, P. Gao, and Y. Ding, "An Analytical Dynamic Model for Vibration Suppression of a Multi-Span Continuous Bridge by Tuned Mass Dampers," *Journal of Marine Science and Engineering*, vol. 11, no. 5, p. 1017, May 2023, doi: 10.3390/jmse11051017.

[10] A. A. Meibodi, N. A. Alexander, J. A. Norman, and A. J. Crewe, "A theoretical and experimental exploration of the seismic dynamics of multi-span bridges," *Bulletin of Earthquake Engineering*, vol. 18, no. 9, pp. 4275–4298, Jul. 2020, doi: 10.1007/s10518-020-00864-6.

[11] K. A. V. Ilyichev, V.A., Nikiforova N.S., "A settlement calculation for neighbouring buildings with mitigation measures upon underground construction," 2017.

[12] S.V. Medvedev, *Engineering seismology*. 1965.

[13] T. R. Rashidov and D. A. Bekmirzaev, "Numerical methods in the study of seismic dynamics of complex systems of underground pipelines," *Izvestiya MGTU MAMI*, vol. 9, no. 4–4, pp. 100–105, Aug. 2015, doi: 10.17816/2074-0530-67073.

[14] A. M. UZDIN, L. N. SMIRNOVA, H. R. ZAINULABIDOVA, SH. SH. NAZAROVA, A. A. DOLGAYA, and A. A. NAZAROV, "THE EFFICIENCY OF SEISMIC ISOLATION DEPENDING ON THE TYPE OF DAMPER," *Structural Mechanics and Analysis of Constructions*, no. 5, pp. 45–53, Oct. 2025, doi: 10.37538/0039-2383.2025.5.45.58.

[15] O. Fusakichi, "On the After-shocks of Earthquakes," *College of Science, Imperial University*, 1894.

[16] M. D. Trifunac, "Biot response spectrum," *Soil Dynamics and Earthquake Engineering*, vol. 26, no. 6–7, pp. 491–500, Jun. 2006, doi: 10.1016/j.soildyn.2006.01.004.

[17] A. I. Lawal, "A new modification to Mononobe-Okabe's pseudo-static model for passive earth pressure prediction using homogeneous differential equation," *Mechanics Research Communications*, vol. 116, p. 103760, Sep. 2021, doi: 10.1016/j.mechrescom.2021.103760.

[18] Y. F. Chen, "Rational and practical method for determination of seismic-induced earth pressure on non-yielding walls," *Journal of Structural Integrity and Maintenance*, vol. 2, no. 1, pp. 48–59, Jan. 2017, doi: 10.1080/24705314.2017.1280587.

[19] V. A. Ismailov, S. I. Yodgorov, A. S. Khusomiddinov, E. M. Yadigarov, B. U. Aktamov, and S. B. Avazov, "Regional seismic risk assessment based on ground conditions in Uzbekistan," *Natural Hazards and Earth System Sciences*, vol. 24, no. 6, pp. 2133–2146, Jun. 2024, doi: 10.5194/nhess-24-2133-2024.

[20] X. Chen, H. Ding, and C. Li, "A quasi-tuned-mass-damper design concept for mitigating the dynamic displacement demand of tall piers," *Soil Dynamics and Earthquake Engineering*, vol. 155, p. 107172, Apr. 2022, doi: 10.1016/j.soildyn.2022.107172.

[21] P. Casini and F. Vestroni, "Mitigation of Structural Vibrations of MDOF Oscillators by Modal Coupling Due to Hysteretic Dampers," *Applied Sciences*, vol. 12, no. 19, p. 10079, Oct. 2022, doi: 10.3390/app121910079.

[22] A. Uzdin, U. Shermukhamedov, Z. Rakhimjonov, and D. Gulomov, "Amplitude-frequency response of seismic-isolated highway bridges at different combinations of span links," 2025, p. 030003. doi: 10.1063/5.0265098.